

Fast variability of TeV γ -rays from the radio galaxy M 87

F. Aharonian¹, A.G. Akhperjanian², A.R. Bazer-Bachi³, M. Beilicke^{4*}, W. Benbow¹,
D. Berge¹, K. Bernlöhr^{1,5}, C. Boisson⁶, O. Bolz¹, V. Borrel³, I. Braun¹,
A.M. Brown⁷, R. Bühler¹, I. Büsching⁸, S. Carrigan¹, P.M. Chadwick⁷,
L.-M. Chounet⁹, G. Coignet¹⁰, R. Cornils⁴, L. Costamante^{1,23}, B. Degrange⁹,
H.J. Dickinson⁷, A. Djannati-Atai¹¹, L.O'C. Drury¹², G. Dubus⁹, K. Egberts¹,
D. Emmanoulopoulos¹³, P. Espigat¹¹, F. Feinstein¹⁴, E. Ferrero¹³, A. Fiasson¹⁴,
G. Fontaine⁹, Seb. Funk⁵, S. Funk¹, M. Füßling⁵, Y.A. Gallant¹⁴, B. Giebels⁹,
J.F. Glicenstein¹⁵, P. Goret¹⁵, C. Hadjichristidis⁷, D. Hauser¹, M. Hauser¹³,
G. Heinzlmann⁴, G. Henri¹⁶, G. Hermann¹, J.A. Hinton^{1,13}, A. Hoffmann¹⁷,
W. Hofmann¹, M. Holleran⁸, S. Hoppe¹, D. Horns¹⁷, A. Jacholkowska¹⁴,
O.C. de Jager⁸, E. Kendziorra¹⁷, M. Kerschhaggl⁵, B. Khélifi^{9,1}, Nu. Komin¹⁴,
A. Konopelko^{5,‡}, K. Kosack¹, G. Lamanna¹⁰, I.J. Latham⁷, R. Le Gallou⁷,
A. Lemièrre¹¹, M. Lemoine-Goumard⁹, J.-P. Lenain⁶, T. Lohse⁵, J.M. Martin⁶,
O. Martineau-Huynh¹⁸, A. Marcowith³, C. Masterson^{1,23}, G. Maurin¹¹,
T.J.L. McComb⁷, E. Moulin¹⁴, M. de Naurois¹⁸, D. Nedbal¹⁹, S.J. Nolan⁷,
A. Noutsos⁷, K.J. Orford⁷, J.L. Osborne⁷, M. Ouchrif^{18,23}, M. Panter¹,
G. Pelletier¹⁶, S. Pita¹¹, G. Pühlhofer¹³, M. Punch¹¹, S. Ranchon¹⁰,
B.C. Raubenheimer⁸, M. Raue⁴, S.M. Rayner⁷, A. Reimer²⁰, J. Ripken⁴,
L. Rob¹⁹, L. Rolland¹⁵, S. Rosier-Lees¹⁰, G. Rowell¹, V. Sahakian²,
A. Santangelo¹⁷, L. Saugé¹⁶, S. Schlenker⁵, R. Schlickeiser²⁰, R. Schröder²⁰,
U. Schwanke⁵, S. Schwarzburg¹⁷, S. Schwemmer¹³, A. Shalchi²⁰, H. Sol⁶,
D. Spangler⁷, F. Spanier²⁰, R. Steenkamp²¹, C. Stegmann²², G. Superina⁹,
P.H. Tam¹³, J.-P. Tavernet¹⁸, R. Terrier¹¹, M. Tluczykont^{9,23}, C. van Eldik¹,
G. Vasileiadis¹⁴, C. Venter⁸, J.P. Vialle¹⁰, P. Vincent¹⁸, H.J. Völk¹,
S.J. Wagner¹³, M. Ward⁷

*To whom correspondence should be addressed; E-mail: matthias.beilicke@desy.de

1. Max-Planck-Institut für Kernphysik, P.O. Box 103980, D 69029 Heidelberg, Germany
2. Yerevan Physics Institute, 2 Alikhanian Brothers St., 375036 Yerevan, Armenia
3. Centre d'Etude Spatiale des Rayonnements, CNRS/UPS, 9 av. du Colonel Roche, BP 4346, F-31029 Toulouse Cedex 4, France
4. Universität Hamburg, Institut für Experimentalphysik, Luruper Chaussee 149, D 22761 Hamburg, Germany
5. Institut für Physik, Humboldt-Universität zu Berlin, Newtonstr. 15, D 12489 Berlin, Germany
6. LUTH, UMR 8102 du CNRS, Observatoire de Paris, Section de Meudon, F-92195 Meudon Cedex, France
7. University of Durham, Department of Physics, South Road, Durham DH1 3LE, U.K.
8. Unit for Space Physics, North-West University, Potchefstroom 2520, South Africa
9. Laboratoire Leprince-Ringuet, IN2P3/CNRS, Ecole Polytechnique, F-91128 Palaiseau, France
10. Laboratoire d'Annecy-le-Vieux de Physique des Particules, IN2P3/CNRS, 9 Chemin de Bellevue - BP 110 F-74941 Annecy-le-Vieux Cedex, France
11. APC, 11 Place Marcelin Berthelot, F-75231 Paris Cedex 05, France[†]
12. Dublin Institute for Advanced Studies, 5 Merrion Square, Dublin 2, Ireland
13. Landessternwarte, Universität Heidelberg, Königstuhl, D 69117 Heidelberg, Germany
14. Laboratoire de Physique Théorique et Astroparticules, IN2P3/CNRS, Université Montpellier II, CC 70, Place Eugène Bataillon, F-34095 Montpellier Cedex 5, France
15. DAPNIA/DSM/CEA, CE Saclay, F-91191 Gif-sur-Yvette, Cedex, France
16. Laboratoire d'Astrophysique de Grenoble, INSU/CNRS, Université Joseph Fourier, BP 53, F-38041 Grenoble Cedex 9, France
17. Institut für Astronomie und Astrophysik, Universität Tübingen, Sand 1, D 72076 Tübingen, Germany
18. Laboratoire de Physique Nucléaire et de Hautes Energies, IN2P3/CNRS, Universités Paris VI & VII, 4 Place Jussieu, F-75252 Paris Cedex 5, France
19. Institute of Particle and Nuclear Physics, Charles University, V Holesovickach 2, 180 00 Prague 8, Czech Republic
20. Institut für Theoretische Physik, Lehrstuhl IV: Weltraum und Astrophysik, Ruhr-Universität Bochum, D 44780 Bochum, Germany
21. University of Namibia, Private Bag 13301, Windhoek, Namibia
22. Universität Erlangen-Nürnberg, Physikalisches Institut, Erwin-Rommel-Str. 1, D 91058 Erlangen, Germany
23. European Associated Laboratory for Gamma-Ray Astronomy, jointly supported by CNRS and MPG

[†] UMR 7164 (CNRS, Université Paris VII, CEA, Observatoire de Paris)

[‡] now at Purdue University, Department of Physics, 525 Northwestern Avenue, West Lafayette, IN 47907-2036, USA

The detection of fast variations of the TeV (10^{12} eV) γ -ray flux, on time-scales of days, from the nearby radio galaxy M 87 is reported. These variations are ~ 10 times faster than that observed in any other waveband and imply a very compact emission region with a dimension similar to the Schwarzschild radius of the central black hole. We thus can exclude several other sites and processes of the γ -ray production. The observations confirm that TeV γ -rays are emitted by extragalactic sources other than blazars, where jets are not relativistically beamed towards the observer.

So far the only extragalactic objects known to emit γ -radiation up to energies of Tera electron volts ($1 \text{ TeV} = 10^{12} \text{ eV}$) are blazars. These are active galactic nuclei (AGN) with a plasma jet emanating from the vicinity of the black hole and pointing close to the observer's line of sight. Due to the bulk relativistic motion of the plasma in the jet the energy and luminosity of emitted photons are boosted by relativistic effects, making blazars detectable up to TeV energies.

The nearby radio galaxy M 87 is located in the Virgo cluster of galaxies at a distance of $\sim 16 \text{ Mpc}$ ($z = 0.0043$) and hosts a central black hole of $(3.2 \pm 0.9) \times 10^9$ solar masses (1). The 2 kpc scale plasma jet (2) originating from the centre of M 87 is resolved at different wavelengths (radio, optical and X-rays). The observed inclination of the jet, at an angle of $\sim 30^\circ$ relative to the observer's line of sight (3), demonstrates that M 87 is not a blazar and hence would represent a new class of TeV γ -ray emitters. M 87 has also been suggested as an accelerator of the enigmatic ultra-high-energy (10^{20} eV) cosmic rays (4,5). Previously, weak evidence for $E > 730 \text{ GeV}$ γ -ray emission from M 87 in 1998/1999 with a statistical significance of 4.1 standard deviations was reported by the High Energy Gamma Ray Astronomy (HEGRA) collaboration (6). No significant emission above 400 GeV was observed by the Whipple collaboration (7) from 2000-2003.

The observations reported here were performed with the High Energy Stereoscopic System (H.E.S.S.) located in Namibia. H.E.S.S. is an array of four imaging atmospheric-Cherenkov telescopes used for the measurement of cosmic γ -rays of energies between 100 GeV and several 10 TeV, see (8) for more details. The observations of M 87 were performed between 2003 and 2006 yielding a total of 89 hours of data after quality selection cuts. After calibration (S2), the H.E.S.S. standard analysis was applied to the data using hard event selection cuts (S1). More information about the standard analysis, as well as a more recent, alternative analysis technique (S3) which gives consistent results, can be found in (12).

An excess of 243 γ -ray events is measured from the direction of M 87 in the whole dataset, corresponding to a statistical significance of 13 standard deviations, establishing M 87 as a TeV γ -ray source (Fig. 1). The position of the excess (Right Ascension α and Declination δ) was found to be $\alpha = 12^{\text{h}}30^{\text{m}}47.2^{\text{s}} \pm 1.4^{\text{s}}$, $\delta = +12^\circ 23' 51'' \pm 19''$ (J2000.0). This is, within the quoted statistical error and the systematic pointing uncertainty of the H.E.S.S. telescopes ($\sim 20''$ in both the Right Ascension and Declination directions) compatible with the nominal (radio) position (13) of the nucleus of M 87 ($\alpha = 12^{\text{h}}30^{\text{m}}49.4^{\text{s}}$, $\delta = +12^\circ 23' 28''$). Considering

the angular resolution of H.E.S.S., the source is consistent with a point-like object with an upper limit for a Gaussian surface-brightness profile of 3 arcmin (99.9% confidence level). At the distance of M 87 (16 Mpc) this corresponds to a radial extension of 13.7 kpc which can be compared with the large-scale structure of M 87 as seen at radio wavelengths (Fig. 1). A $\sim 10^6$ times stronger constraint on the size of the TeV emission region is deduced from the observed short-term flux variability, as shown below.

The differential energy spectra obtained for the 2004 and 2005 data sets (Fig. 2) are both well fit by a power-law function $dN/dE \propto E^{-\Gamma}$. The spectrum measured in 2005 is found to be hard ($\Gamma \sim 2.2$) and reaches beyond 10 TeV with an average γ -ray flux of a factor of ~ 5 higher than in 2004.

The total γ -ray flux above 730 GeV (Fig. 3) for the individual years from 2003 to 2006 indicates variability on a yearly basis (14) corresponding to a statistical significance of 3.2 standard deviations, being derived from a χ^2 fit of a constant function. The variability is confirmed by a Kolmogorov test comparing the distribution of photon arrival times to the distribution of background arrival times yielding a statistical significance for burst-like (non-constant) behaviour of the source of 4.5 standard deviations. Surprisingly variability on time-scales of days (flux doubling) was found in the high state data of 2005 (Fig. 3, upper panel) with a statistical significance of more than 4 standard deviations. This is the fastest variability observed in any waveband from M 87 and strongly constrains the size of the emission region of the TeV γ -radiation, which is further discussed below. No indications for short-term variability were found in the data of 2003, 2004 and 2006, which is not unexpected given the generally lower statistical significances of the γ -ray excesses in those years.

These observational results (location, spectrum & variability) challenge most scenarios of very-high-energy γ -ray production in extragalactic sources. Although the luminosity ($\approx 3 \times 10^{40}$ erg/s) of TeV γ -rays is quite modest and does not cause any problems with the global energy budget of the active galaxy M 87, several models can be dismissed. The upper limit on the angular size of ~ 3 arcmin (13.7 kpc $\approx 4.3 \cdot 10^{22}$ cm) centred on the M 87 nucleus position already excludes the core of the Virgo cluster (15) and outer radio regions of M 87 as TeV γ -ray emitting zones. Further, the observed variability on time-scales of $\Delta t \sim 2$ days requires a very compact emission region due to the light-crossing time. The characteristic size is limited to $R \leq c \cdot \Delta t \cdot \delta \approx 5 \times 10^{15} \delta$ cm $\approx 5 \times \delta R_s$, where δ is the relativistic Doppler factor (16) of the source of TeV radiation and $R_s \approx 10^{15}$ cm is the Schwarzschild radius of the M 87 supermassive black hole (see below). For any reasonable value of the Doppler factor (i.e. $1 < \delta < 50$, as used in the modelling of TeV γ -ray blazars), this implies a drastic constraint on the size of the TeV γ -ray source which immediately excludes several potential sites and hypotheses of γ -ray production. First of all this concerns the elliptical galaxy M 87 (15) and the γ -ray production due to dark matter annihilation (17). The most obvious candidate for efficient particle acceleration (18), namely the entire extended kiloparsec jet, is also excluded. Although compatible with the TeV source position, even the brightest knot in the jet (knot A) appears excluded with its typical size of the order of one arcsec (about 80 pc $\approx 2.5 \cdot 10^{20}$ cm) resolved in the X-ray range (19).

An interesting possibility would be the peculiar knot (HST-1) in the jet of M 87 (see supporting online text and Fig. S2), a region of many violent events, with X-ray flares exceeding the luminosity of the core emission (*S4*) and super-luminal blobs being detected downstream. Modelling the high-energy radiation properties of this region (by synchrotron and inverse-Compton scenarios), several authors favour sizes in the range of 0.1 to 1 pc (for moderate values of the Doppler factor ranging between 2 and 5) (*21, 22, S4*). But, formally there is no robust lower limit on the size of HST-1, therefore we cannot exclude HST-1 as a source of TeV γ -rays. However, it would be hard to realize the short-term variability of the TeV γ -ray emission in relation to HST-1, at least within the framework of current models. While the size of the γ -ray production region does not exceed $R \leq 5 \times 10^{15} \delta$ cm, the location of HST-1 along the jet at 0.85 arcsec from the nucleus, which corresponds to $d \approx 65$ pc, implies that the energy would be channelled from the central object into the γ -ray production region within an unrealistically small opening angle $\sim R/d \approx 1.5 \times 10^{-3} \delta$ degree.

The only remaining and promising possibility is to conclude that the site of TeV γ -ray production is the nucleus of M 87 itself (*23*). In contrast to the established TeV γ -ray blazars, the large scale jet of M 87 is seen at a relatively large jet angle ($\theta \sim 30^\circ$) which suggests a quite modest Doppler boosting of its radiation. Nevertheless, due to the proximity of M 87, both leptonic (*24*) and hadronic (*5, 25*) models predicted detectable TeV γ -ray emission. However, these scenarios typically produce a soft energy spectrum of TeV γ -rays, clearly in contrast to the hard spectrum measured by H.E.S.S. Leptonic models can be adapted in various ways to match the new results. Within synchrotron-self-Compton (SSC) scenarios (*26*), one method is to consider the possibility of differential Doppler-boosting in the jet near the core region, a phenomenon clearly expected in the jet formation zone which extends over less than 0.1 pc from the nucleus (*27*). Emitting plasma blobs of small sizes with Doppler factors between 5 and 30 and magnetic fields well below equipartition can account for the observed TeV γ -ray emission. An additional flux contribution from inverse-Compton scattering of background photons, coming from scattered disk emission or from dust, can further reduce the range of Doppler factors towards moderate values.

The TeV γ -ray photons (independent of their production mechanism) might be absorbed by the pair absorption process $\gamma_{\text{TeV}} + \gamma_{\text{IR}} \rightarrow e^+e^-$ on the local infrared (IR) radiation field in the TeV γ -ray emission region. Since no signature for an absorption can be identified in the energy spectrum up to 10 TeV, one can derive an upper limit on the luminosity of the infrared radiation field at 0.1 eV (corresponding to a wavelength of approximately 10 micron, most relevant for absorption of 10 TeV γ -rays) to be $L(0.1 \text{ eV}) \leq 3.6 \times 10^{38} (R/10^{15} \text{ cm}) \text{ erg/s}$, where R is the size of the TeV γ -ray emission region. Such a low central IR radiation luminosity supports the hypothesis of an advection-dominated accretion disk (i.e. an accretion disk with low radiative efficiency) in M 87 (*28*) and generally excludes a strong contribution of external inverse-Compton emission on IR light to the TeV γ -ray flux.

If one accepts the hypothesis that protons can be accelerated as high as 10^{20} eV in jets of radio galaxies, then (hadronic) proton synchrotron models (*5, 25*) can not be excluded considering the presented data. An alternative γ -ray production mechanism is curvature radiation of ultra-

high-energy protons in the immediate vicinity of the supermassive black hole. This novel mechanism can simultaneously explain both the hard spectrum and fast variability of the observed TeV γ -ray emission. Rapidly rotating black holes embedded in externally supported magnetic fields can generate electric fields and accelerate protons to energies up to 10^{20} eV (29, 30, 31). Assuming that acceleration of protons takes place effectively within 3 Schwarzschild radii R_s , and if the horizon threading magnetic field is not much below 10^4 G, one should expect γ -ray radiation due to proton curvature radiation extending to at least 10 TeV (the electron curvature radiation is less likely because of severe energy losses even in a tiny component of an irregular magnetic field). No correlation with fluxes at other wavelengths is expected in this model. Although the size of the γ -ray production region, $R \sim 3R_s \sim 3 \times 10^{15}$ cm perfectly matches the observed variability scale, and the model allows extension of the γ -ray spectrum to 10 TeV without any significant correlation at other wavelength, the main problem of the model is the suggested magnetic field. It is orders of magnitude larger than the B-field expected from the accretion process, given the very low accretion rate as it follows from the bolometric luminosity of the core as well as the estimates of the power of the jet in M 87.

In summary, the time-scale of the short-term variability of the TeV γ -rays is in the order of the light crossing time of the black hole (located at the center of M 87), which is a natural time-scale of the object. Therefore, the results reported here give clear evidence for the production of TeV γ -rays in the immediate vicinity of the black hole of M 87.

References and Notes

1. F. Macchetto et al., *Astroph. J.* **489**, 579 (1997).
2. H.L. Marshall et al., *Astroph. J.* **564**, 683 (2002).
3. G.V. Bicknell, M.C. Begelman, *Astroph. J.* **467**, 597 (1996).
4. P.L. Biermann et al., *Nucl. Phys. B, Proc. Suppl.* **87**, 417 (2000).
5. R.J. Protheroe et al., *Astropart. Phys.* **19**, Issue 4, 559 (2003).
6. F. Aharonian et al. (HEGRA collab.), *Astron. Astrophys.* **403**, L1 (2003).
7. S. Le Bohec et al., *Astroph. J.* **610**, 156 (2004).
8. W. Hofmann, *Proc. of the 29th International Cosmic Ray Conference (Pune)*, **10**, 97 (2005).
9. F. Aharonian et al. (H.E.S.S. collab.), *Astropart. Phys.* **22**, 109 (2004).
10. W. Benbow, *Proceedings 'Towards a network of atmospheric Cherenkov detectors VII' (Palaiseau)*, p. 163 (2005).

11. M. de Naurois, *Proceedings 'Towards a network of atmospheric Cherenkov detectors VII' (Palaiseau)*, 149 (2005), see astro-ph/0607247.
12. Materials and methods are available as supporting material on Science Online.
13. C. Ma et al., *Astronom. J.* **116**, 516 (1998).
14. M. Beilicke et al., *Proc. of TEXAS Symposium on Relativistic Astrophysics (Stanford University)*, Paper #2403 (2004), see astro-ph/0504395.
15. C. Pfrommer, T.A. Enßlin, *Astron. Astrophys.* **407**, L73 (2003).
16. Emission from a region which is moving with a relativistic speed $\beta = v/c$ (c is the speed of light) is boosted along the direction of movement (relativistic beaming). The boost is a function of the observation angle θ relative to this direction and is described by the Doppler factor $\delta = (\Gamma(1 - \beta \cos \theta))^{-1}$, where $\Gamma = (1 - \beta^2)^{-1/2}$ is the Lorentz factor of the emission region.
17. E.A. Baltz et al., *Phys. Rev. D* **61**, 3514 (2000).
18. L. Stawarz et al., *Astroph. J.* **626**, 120 (2005).
19. E.S. Perlman, A.S. Wilson, *Astroph. J.* **627**, 140 (2005).
20. D.E. Harris et al., *Astroph. J.* **640**, 211 (2006).
21. D.E. Harris, et al., *Astroph. J.* **586**, L41 (2003).
22. L. Stawarz, et al., *MNRAS* **370**, 981 (2006).
23. W. Forman, et al., *Astroph. J.* **635**, 894 (2005).
24. M. Georganopoulos et al., *Astroph. J.* **634**, L33 (2005).
25. A. Reimer et al., *Astron. Astrophys.* **419**, 89 (2004).
26. D.L. Band, J.E. Grindlay, *Astroph. J.* **308**, 576 (1986).
27. W. Junor, J.A. Biretta, M. Livio *Nature* **401**, 891 (1999).
28. C.S. Reynolds, T. di Matteo, A.C. Fabian, U. Hwang, C.R. Canizares, *MNRAS* **283**, L111 (1996).
29. A. Levinson, *Phys. Rev. Lett.* **85**, 912 (2000).
30. E. Boldt, M. Loewenstein, *MNRAS* **316**, 29 (2000).

31. F.A. Aharonian, A.A. Belyanin, E.V. Derishev, V.V. Kocharovskiy, V.I. Kocharovskiy, *Phys. Rev. D* **66**, 023005 (2002).
32. F.N. Owen et al., *Proc. of The universe at low radio frequencies. ASP Conf. Ser.*, 199 (2000), see astro-ph/0006152.
33. provided by D. Harris, private communication.
34. Acknowledgement. The support of the Namibian authorities and of the University of Namibia in facilitating the construction and operation of H.E.S.S. is gratefully acknowledged, as is the support by the German Ministry for Education and Research (BMBF), the Max Planck Society, the French Ministry for Research, the CNRS-IN2P3 and the Astroparticle Interdisciplinary Programme of the CNRS, the U.K. Particle Physics and Astronomy Research Council (PPARC), the IPNP of the Charles University, the South African Department of Science and Technology and National Research Foundation, and by the University of Namibia. We thank D. Harris for providing the Chandra X-ray light curve of the M 87 nucleus.

Supporting Online Material

www.sciencemag.org
Materials and Methods
Supporting text
Figs. S1, S2
Tab. S1
References

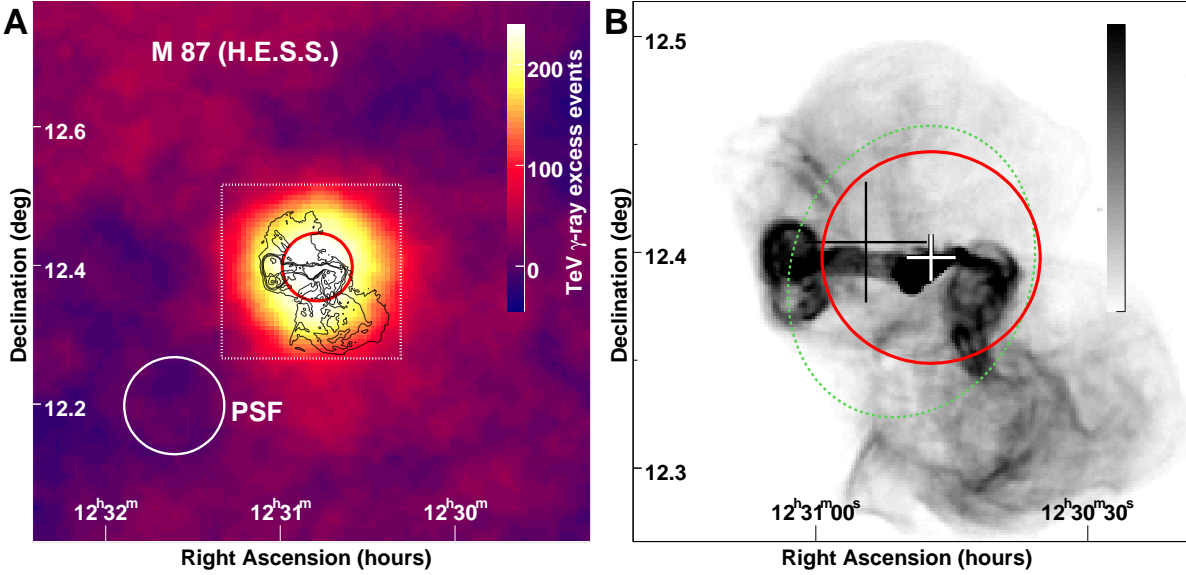


Fig. 1. Shown are the sky map as well as the position and extension limit of the TeV γ -ray emission from M 87. (A) Smoothed TeV γ -ray excess map (color coded, 0.1° integration radius) as measured by H.E.S.S. The size (68% containment radius) of the H.E.S.S. point spread function (PSF) is also indicated. The red circle indicates the intrinsic extension upper limit (99.9% confidence level) of 3 arcmin of the TeV γ -ray excess corresponding to 13.7 kpc in M 87. The contour lines show the 90 cm radio emission (32). The white box marks the cut-out shown in the right panel. (B) The 90 cm radio data (32) measured with the Very Large Array, together with the TeV position with statistical and $20''$ pointing uncertainty errors (white cross) and again the 99.9% c.l. extension upper limit (red circle). Note that the size of the emission region deduced from the short-term variability is $\sim 10^6$ times smaller. The black cross marks the position and statistical error of the γ -ray source reported by HEGRA. The green ellipse indicates the host galaxy seen in the optical wavelengths with an extension of 8.3×6.6 arcmin in diameter.

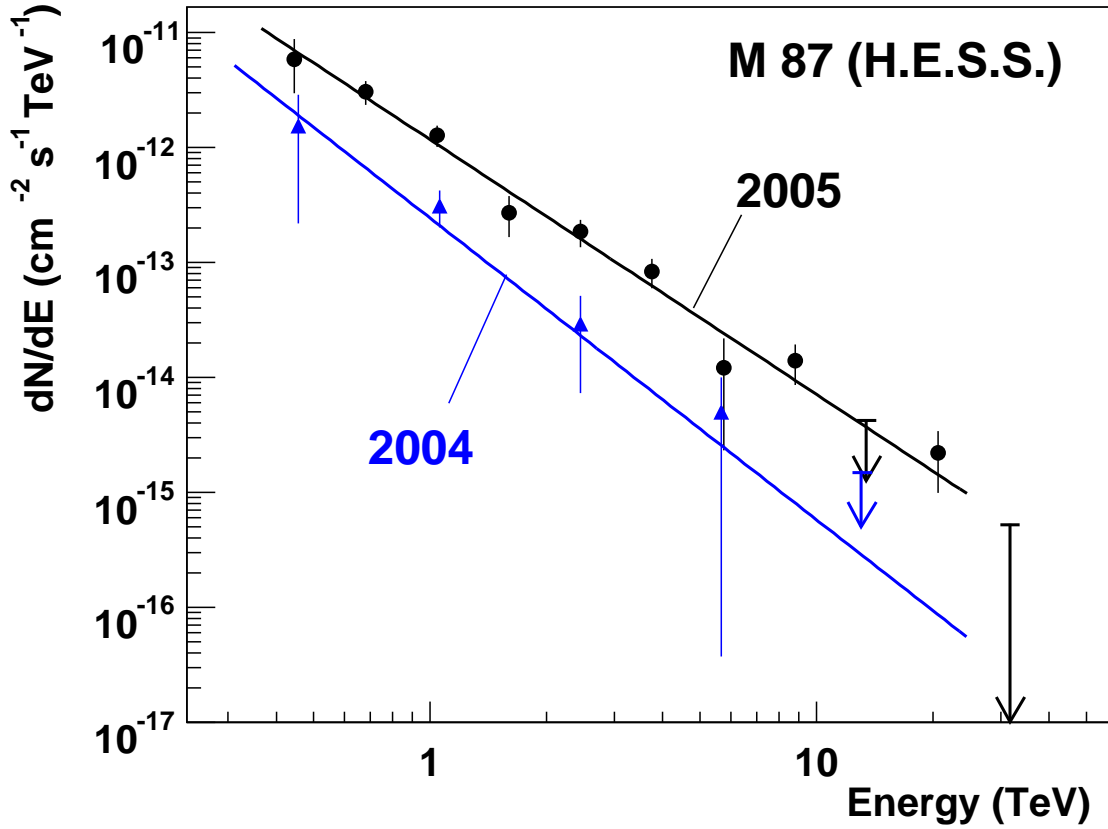


Fig. 2. The differential energy spectrum of M 87 obtained from the 2004 and the 2005 data (using standard event selection cuts (*SI*)) covering a range of ~ 400 GeV to ~ 10 TeV. Spectra for the 2003 and 2006 data sets could not be derived due to limited event statistics. Flux points with a statistical significance less than 1.5 standard deviations are given as upper limits (99.9% c.l.). The corresponding fits of a power-law function $dN/dE = I_0 \cdot (E/1 \text{ TeV})^{-\Gamma}$ are indicated as lines. The photon indices are $\Gamma = 2.62 \pm 0.35$ (2004 data) and $\Gamma = 2.22 \pm 0.15$ (2005 data). Aside from the difference in the flux normalisation by a factor of ~ 5 ($I_0 = (2.43 \pm 0.75) \times 10^{-13} \text{ cm}^{-2} \text{ s}^{-1} \text{ TeV}^{-1}$ in 2004 and $I_0 = (11.7 \pm 1.6) \times 10^{-13} \text{ cm}^{-2} \text{ s}^{-1} \text{ TeV}^{-1}$ in 2005) no variation in spectral shape is found within errors. The systematic error on the photon index and flux normalisation are estimated to be $\Delta\Gamma = 0.1$, and $\Delta I_0/I_0 = 0.2$, respectively.

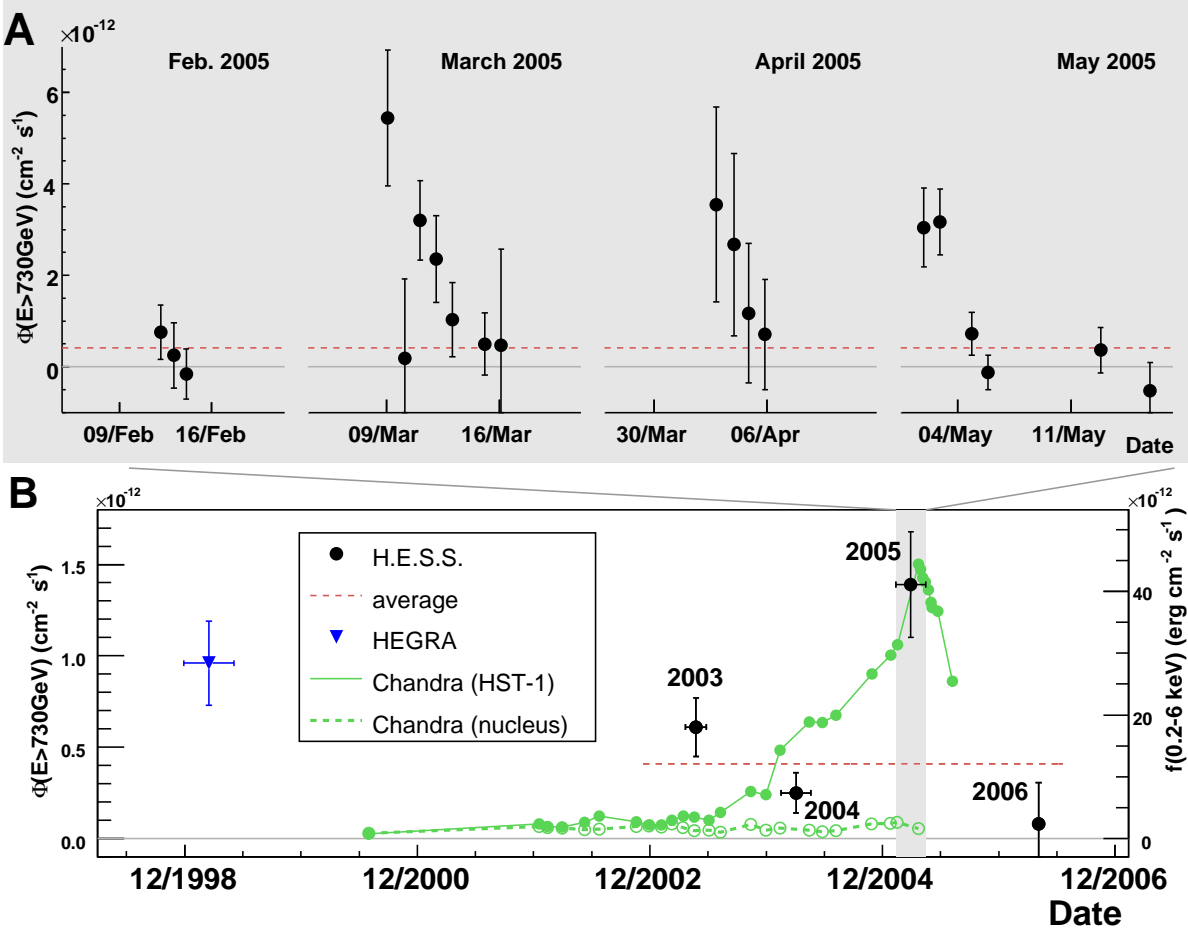


Fig. 3. Gamma-ray flux above an energy of 730 GeV as a function of time. The given error bars correspond to statistical errors. (B) The average flux values for the years 2003 to 2006 as measured with H.E.S.S. together with a fit of a constant function (red line). The flux reported by HEGRA is also drawn (a systematic error must be taken into account when comparing results from the two instruments). (A) The night-by-night fluxes for the four individual months (February to May) of the high-state measurements in 2005 with significant variability on (flux doubling) time-scales of ~ 2 days. The green points in (B) correspond to the 0.2 – 6 keV X-ray flux of the knot HST-1 (solid, $S4$) and the nucleus (dashed, 33) as measured by Chandra; the lines are linear interpolations of the flux points. No unique correlation between the flux of X-rays and TeV γ -rays can be identified (the X-ray/TeV data were not taken simultaneously).

Supporting Materials and methods

*To whom correspondence should be addressed;

E-mail: matthias.beilicke@desy.de, Olivier.Martineau-Huynh@lpnhep.in2p3.fr

H.E.S.S. observations and standard analysis

When a primary γ -ray photon (or hadron) of TeV energies enters the earth's atmosphere, an extended air shower consisting of millions of secondary particles develops in the atmosphere. The Cherenkov light which is emitted in the air shower is recorded by the photomultiplier camera situated in the focal plane of each H.E.S.S. Cherenkov telescope. The recorded images of the shower are parameterized using a set of parameters (referred to as Hillas parameters) and are used to reconstruct for example the energy and direction of the primary particle. The geometrical width of an image is scaled using an expectation value for the corresponding observation conditions (zenith angle, shower distance, etc.) and is used to distinguish between γ -ray and hadron induced showers. This procedure is referred to as the H.E.S.S. standard analysis and is described in more detail elsewhere (*S1*). The simultaneous recording with up to four telescopes (stereoscopic observation) with this new generation experiment allows an improved (as compared to single telescope observations) event-by-event measurement of the direction ($\Delta\theta \sim 0.1^\circ$) and energy ($\Delta E/E \approx 15\%$) as well as a superior background suppression of charged cosmic rays. Hard event selection cuts have been used in the analysis reported here providing an optimum background rejection for sources with hard energy spectra at some expense of a lower event rate and an increased energy threshold of 640 GeV for the average zenith angle of 40° of the M87 observations. The energy spectrum was derived using the standard cuts with a lower threshold of ~ 400 GeV for the same zenith angle.

The H.E.S.S. observations of M87 were performed between 2003 and 2006 for a total of 89 hours after data quality selection cuts (Tab. S1). The 2003 data (~ 25 h) were taken with only two operational telescopes during the construction phase, while the measurements of the following years have been performed with the full four telescope array which has a twice better sensitivity as compared to the two-telescope setup. Therefore, the energy spectra and the sky position and extension limit of the TeV γ -ray excess were derived from the 2004-2006 data only. Generating an energy spectrum from the 2006 data was not possible due to the very limited event statistics.

Application of an alternative analysis method

The results have been cross-checked with a recently developed alternative analysis method. Beside an independent calibration of the H.E.S.S. raw data (*S2*), this technique is based on the combination of a parameterisation of the shower images using the moment method of Hillas (similar to the one described above), and the technique referred to as model analysis (*S3*). This latter method implies a pixel-by-pixel comparison of the shower images (recorded with the

H.E.S.S. photomultiplier cameras) with a template generated by a semi-analytical shower development model. The γ -ray primary energy, direction and impact position are obtained by maximising a log-likelihood function associated with this comparison. The model analysis uses all available pixels in the camera, without the requirement of an image cleaning. Since the background rejection is based on independent variables in these two methods, their combination in this alternative analysis improves the background rejection. The combined analysis used here therefore yields more significant results than the Hillas parameter based standard analysis alone.

The light curve of the 2005 flux high state of M 87, in which the short-term variability is identified, obtained with this alternative analysis method is shown in Fig. S1. The corresponding significance of the short-term variability is above 6 standard deviations, clearly confirming the results obtained from the standard analysis described in the main text. The energy spectra ($\Gamma = 2.61 \pm 0.24$, $I_0 = (3.60 \pm 0.57) \times 10^{-13} \text{ cm}^{-2} \text{ s}^{-1} \text{ TeV}^{-1}$ for the 2004 data and $\Gamma = 2.20 \pm 0.09$, $I_0 = (13.9 \pm 1.2) \times 10^{-13} \text{ cm}^{-2} \text{ s}^{-1} \text{ TeV}^{-1}$ for the 2005 data) as well as the sky position of $\alpha = 12^{\text{h}}30^{\text{m}}50.0^{\text{s}} \pm 1.3^{\text{s}}$ and $\delta = +12^{\circ}23'53'' \pm 19''$ (J2000.0) and extension limit of 3 arcmin of the TeV γ -ray excess are also compatible with the results of the standard analysis.

The peculiar knot HST-1

HST-1 is the innermost resolved knot in the jet of M 87 (Fig. S2). Up to now, no extension or substructure of HST-1 could be resolved in the X-ray range. This region is the site of many violent events, with X-ray flares exceeding the luminosity of the core emission and super-luminal blobs being detected downstream. The radio, UV and X-ray fluxes (*S4*) of HST-1 have increased by more than a factor of 50 over the period from 2000 to 2005 (Fig. 3). In addition, isolated flares with variability on time-scales of about 1 month have been detected both in optical (*S5*) and X-ray (*S4*) energy bands.

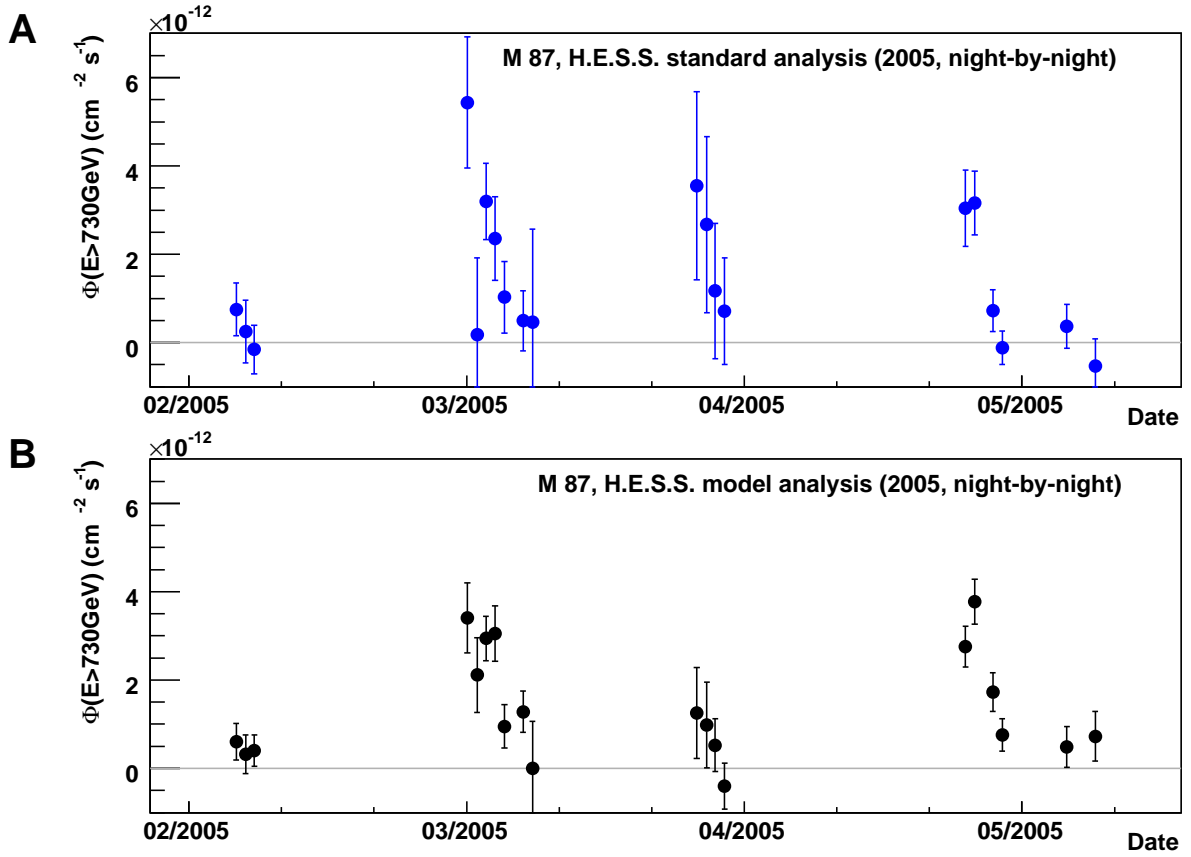


Fig. S1. Gamma-ray flux above an energy of 730 GeV as a function of time for the 2005 high state (February to May) from the two analysis methods in comparison. The given error bars correspond to statistical errors. (A) The results of the standard analysis shown in Fig. 3, whereas (B) shows the fluxes obtained using the model analysis (*S3*), including an independent calibration chain. Due to its higher γ -ray acceptance, about 60% of the γ -ray events obtained from the model analysis are not contained in the corresponding standard analysis in which the hard event selection cuts were used, making the two data sets (partly) statistically independent. Both methods exhibit short-time variability with comparable time-scales.

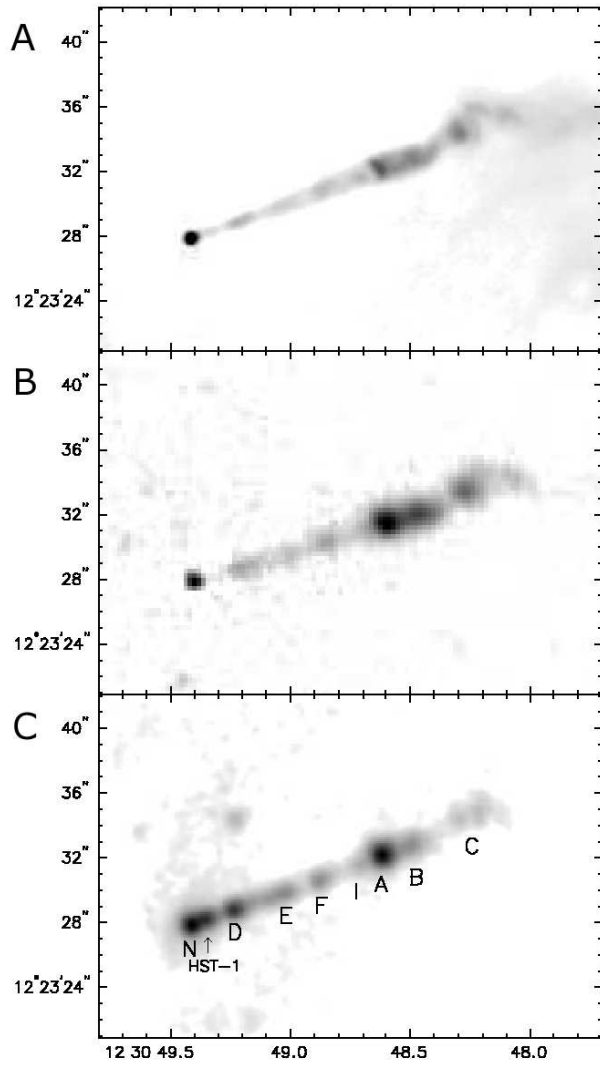


Fig. S2. The central 2 kpc jet of M 87 which is resolved at radio (A), optical (B) and X-ray (C) energies. The nucleus (N), the closest knot HST-1 as well as other knots in the jet are indicated. The image is adopted from (S6).

Tab. S1. Summary of H.E.S.S. observations of M 87. Shown is the time period for each year in which observations were performed, the observation time T_{obs} and T_{live} (corrected for the detector dead time) as well as the number of telescopes in the system. The 2003 data (marked with a *) were taken with only two telescopes in a single operation mode (no stereoscopic trigger) during the construction phase.

Year	time period	T_{obs} [h]	T_{live} [h]	N_{tel}
2003*	24. Apr. - 28. June	25.1	19.2	2
2004	17. Feb. - 23. May	35.2	31.4	4
2005	12. Feb. - 15. May	23.0	21.1	4
2006	25. Apr. - 18. May	5.3	4.8	4

References and Notes

- S1. W. Benbow, *Proceedings 'Towards a network of atmospheric Cherenkov detectors VII' (Palaiseau)*, p. 163 (2005).
- S2. F. Aharonian et al. (H.E.S.S. collab.), *Astropart. Phys.* **22**, 109 (2004).
- S3. M. de Naurois, *Proceedings 'Towards a network of atmospheric Cherenkov detectors VII' (Palaiseau)*, 149 (2005), see astro-ph/0607247.
- S4. D.E. Harris et al., *Astroph. J.* **640**, 211 (2006).
- S5. E.S. Perlman et al., *Astroph. J.* **599**, L65 (2003).
- S6. A.S. Wilson, Y. Yang, *Astroph. J.* **568**, 133 (2002).